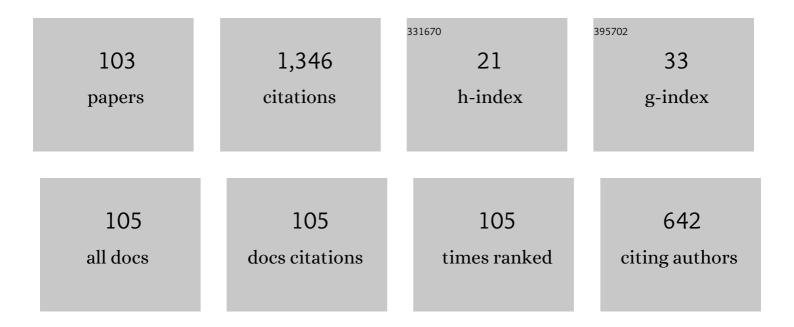
## Tadashi Yamaguchi

List of Publications by Year in descending order

Source: https://exaly.com/author-pdf/10936929/publications.pdf Version: 2024-02-01



#	Article	IF	CITATIONS
1	B-Mode Ultrasound With Algorithm Based on Statistical Analysis of Signals: Evaluation of Liver Fibrosis in Patients With Chronic Hepatitis C. American Journal of Roentgenology, 2009, 193, 1037-1043.	2.2	94
2	A pilot approach for quantitative assessment of liver fibrosis using ultrasound: preliminary results in 79 cases. Journal of Hepatology, 2006, 44, 68-75.	3.7	77
3	Proposal of a parametric imaging method for quantitative diagnosis of liver fibrosis. Journal of Medical Ultrasonics (2001), 2010, 37, 155-166.	1.3	62
4	Estimation of Characteristics of Echo Envelope Using RF Echo Signal from the Liver. Japanese Journal of Applied Physics, 2001, 40, 3900-3904.	1.5	60
5	Estimation of the Scatterer Distribution of the Cirrhotic Liver using Ultrasonic Image. Japanese Journal of Applied Physics, 1998, 37, 3093-3096.	1.5	43
6	Examination of the Spatial Correlation of Statistics Information in the Ultrasonic Echo from Diseased Liver. Japanese Journal of Applied Physics, 2002, 41, 3585-3589.	1.5	43
7	Modeling of the Cirrhotic Liver Considering the Liver Lobule Structure. Japanese Journal of Applied Physics, 1999, 38, 3388-3392.	1.5	38
8	Quantitative Estimation Method for Liver Fibrosis Based on Combination of Rayleigh Distributions. Japanese Journal of Applied Physics, 2010, 49, 07HF06.	1.5	38
9	Stability of Quantitative Evaluation Method of Liver Fibrosis Using Amplitude Distribution Model of Fibrotic Liver. Japanese Journal of Applied Physics, 2011, 50, 07HF17.	1.5	35
10	Three-dimensional quantitative ultrasound for detecting lymph node metastases. Journal of Surgical Research, 2013, 183, 258-269.	1.6	34
11	Liver tissue characterization for each pixel in ultrasound image using multi-Rayleigh model. Japanese Journal of Applied Physics, 2014, 53, 07KF27.	1.5	34
12	Three-Dimensional Model of the Scatterer Distribution in Cirrhotic Liver. Japanese Journal of Applied Physics, 2003, 42, 3292-3298.	1.5	33
13	Speed of sound in diseased liver observed by scanning acoustic microscopy with 80 MHz and 250 MHz. Journal of the Acoustical Society of America, 2016, 139, 512-519.	1.1	32
14	Verification of echo amplitude envelope analysis method in skin tissues for quantitative follow-up of healing ulcers. Japanese Journal of Applied Physics, 2018, 57, 07LF15.	1.5	32
15	Extraction of Quantitative Three-Dimensional Information from Ultrasonic Volumetric Images of Cirrhotic Liver. Japanese Journal of Applied Physics, 2000, 39, 3266-3269.	1.5	30
16	Evaluation of Ultrasonic Fiber Structure Extraction Technique Using Autopsy Specimens of Liver. Japanese Journal of Applied Physics, 2005, 44, 4615-4621.	1.5	30
17	Target Detectability Using Coded Acoustic Signal in Indoor Environments. Japanese Journal of Applied Physics, 2008, 47, 4325-4328.	1.5	30
18	Accuracy of High-Resolution Ultrasound in the Detection of Meniscal Tears and Determination of the Visible Area of Menisci. Journal of Bone and Joint Surgery - Series A, 2015, 97, 799-806.	3.0	30

Тадазні Үамадисні

#	Article	IF	CITATIONS
19	Estimation of scatterer size and acoustic concentration in sound field produced by linear phased array transducer. Japanese Journal of Applied Physics, 2015, 54, 07HF14.	1.5	25
20	Tissue characterization of skin ulcer for bacterial infection by multiple statistical analysis of echo amplitude envelope. Japanese Journal of Applied Physics, 2016, 55, 07KF14.	1.5	24
21	Position detection of small objects in indoor environments using coded acoustic signal. Acoustical Science and Technology, 2008, 29, 15-20.	0.5	23
22	Quantitative US Elastography Can Be Used to Quantify Mechanical and Histologic Tendon Healing in a Rabbit Model of Achilles Tendon Transection. Radiology, 2017, 283, 408-417.	7.3	21
23	Acoustic Impedance Analysis with High-Frequency Ultrasound for Identification of Fatty Acid Species in the Liver. Ultrasound in Medicine and Biology, 2017, 43, 700-711.	1.5	21
24	Modeling the envelope statistics of three-dimensional high-frequency ultrasound echo signals from dissected human lymph nodes. Japanese Journal of Applied Physics, 2014, 53, 07KF22.	1.5	20
25	Water-Filled Laparoendoscopic Surgery (WAFLES): Feasibility Study in Porcine Model. Journal of Laparoendoscopic and Advanced Surgical Techniques - Part A, 2012, 22, 70-75.	1.0	19
26	THE ULTRASONIC THREE-DIMENSIONAL FILTER FOR THE QUANTITATIVE DIAGNOSIS OF LIVER FIBROSIS. Journal of Mechanics in Medicine and Biology, 2009, 09, 579-588.	0.7	18
27	Ultrasound-based lipid content quantification using double Nakagami distribution model in rat liver steatosis. Japanese Journal of Applied Physics, 2020, 59, SKKE23.	1.5	17
28	Stability of Quantitative Evaluation Method of Liver Fibrosis Using Amplitude Distribution Model of Fibrotic Liver. Japanese Journal of Applied Physics, 2011, 50, 07HF17.	1.5	17
29	Application of transcutaneous ultrasonography for the diagnosis of muscle mass loss in patients with liver cirrhosis. Journal of Gastroenterology, 2018, 53, 652-659.	5.1	16
30	Quantitative evaluation method for liver fibrosis based on multi-Rayleigh model with estimation of number of tissue components in ultrasound B-mode image. Japanese Journal of Applied Physics, 2018, 57, 07LF17.	1.5	16
31	Quantitative Evaluation of Liver Fibrosis Using Multi-Rayleigh Model with Hypoechoic Component. Japanese Journal of Applied Physics, 2013, 52, 07HF19.	1.5	15
32	Probability image of tissue characteristics for liver fibrosis using multi-Rayleigh model with removal of nonspeckle signals. Japanese Journal of Applied Physics, 2015, 54, 07HF20.	1.5	15
33	Ultrasound Assessment of Hepatic Steatosis by Using the Double Nakagami Distribution: A Feasibility Study. Diagnostics, 2020, 10, 557.	2.6	15
34	Verification of the influence of liver microstructure on the evaluation of shear wave velocity. Japanese Journal of Applied Physics, 2021, 60, SDDE11.	1.5	15
35	Comprehensive backscattering characteristics analysis for quantitative ultrasound with an annular array: a basic study on homogeneous scattering phantom. Japanese Journal of Applied Physics, 2019, 58, SGGE08.	1.5	12
36	Material Properties of Human Ocular Tissue at 7-µm Resolution. Ultrasonic Imaging, 2017, 39, 313-325.	2.6	11

#	Article	IF	CITATIONS
37	Local Transverse-Slice-Based Level-Set Method for Segmentation of 3-D High-Frequency Ultrasonic Backscatter From Dissected Human Lymph Nodes. IEEE Transactions on Biomedical Engineering, 2017, 64, 1579-1591.	4.2	11
38	Al-Based Radiological Imaging for HCC: Current Status and Future of Ultrasound. Diagnostics, 2021, 11, 292.	2.6	11
39	Speed of sound evaluation considering spatial resolution in a scanning acoustic microscopy system capable of observing wide spatial area. Japanese Journal of Applied Physics, 2020, 59, SKKE13.	1.5	11
40	Basic concept and clinical applications of quantitative ultrasound (QUS) technologies. Journal of Medical Ultrasonics (2001), 2021, 48, 391-402.	1.3	11
41	Proposal of compound amplitude envelope statistical analysis model considering low scatterer concentration. Japanese Journal of Applied Physics, 2018, 57, 07LD19.	1.5	10
42	Improved evaluation of backscatter characteristics of soft tissue using high-frequency annular array. Japanese Journal of Applied Physics, 2020, 59, SKKE17.	1.5	10
43	Analysis of fluctuation for pixel-pair distance in co-occurrence matrix applied to ultrasonic images for diagnosis of liver fibrosis. Journal of Medical Ultrasonics (2001), 2017, 44, 23-35.	1.3	9
44	High-frequency ultrasonic backscatter coefficient analysis considering microscopic acoustic and histopathological properties of lymphedema dermis. Japanese Journal of Applied Physics, 2020, 59, SKKE15.	1.5	9
45	Eradication of esophageal varices by sclerotherapy combined with argon plasma coagulation: Effect of portal hemodynamics and longitudinal clinical course. Digestive Endoscopy, 2016, 28, 152-161.	2.3	8
46	Comparable analysis of bubble translation due to acoustic radiation force based on simultaneous acoustical and optical observation. Japanese Journal of Applied Physics, 2020, 59, SKKE07.	1.5	8
47	Fatty liver evaluation with double-Nakagami model under low-resolution conditions. Japanese Journal of Applied Physics, 2021, 60, SDDE06.	1.5	8
48	The Quantitative Ultrasound Diagnosis of Liver Fibrosis Using Statistical Analysis of the Echo Envelope. , 2013, , 275-288.		8
49	Verification of generated cavitation of an ultrasonically activated scalpel. Choonpa Igaku, 2012, 39, 101-111.	0.0	8
50	Echo envelope analysis method for quantifying heterogeneity of scatterer distribution for tissue characterization of liver fibrosis. , 2010, , .		7
51	Hepatic Filling Rate of a Microbubble Agent: A Novel Predictor of Long-Term Outcomes in Patients With Cirrhosis. Ultrasound in Medicine and Biology, 2014, 40, 2082-2088.	1.5	7
52	Frequency dependence of attenuation and backscatter coefficient of ex vivo human lymphedema dermis. Journal of Medical Ultrasonics (2001), 2020, 47, 25-34.	1.3	7
53	Validation of differences in backscatter coefficients among four ultrasound scanners with different beamforming methods. Journal of Medical Ultrasonics (2001), 2020, 47, 35-46.	1.3	7
54	Experimental analyses of the cavitation generated by ultrasonically activated surgical devices. Surgery Today, 2017, 47, 122-129.	1.5	6

Tadashi Yamaguchi

#	Article	IF	CITATIONS
55	Measurement of shear wave propagation speed by estimation of two-dimensional wavenumbers using phase of particle velocity. Japanese Journal of Applied Physics, 2018, 57, 07LF07.	1.5	6
56	Ultrasound assessment of translation of microbubbles driven by acoustic radiation force in a channel filled with stationary fluid. Journal of the Acoustical Society of America, 2019, 146, 2335-2349.	1.1	6
57	Stability of backscattering coefficient evaluation with clinical ultrasound scanner in homogeneous medium when sound field characteristics differ from reference signal. Japanese Journal of Applied Physics, 2021, 60, SDDE24.	1.5	6
58	A quantitative ultrasound-based method and device for reliably guiding pathologists to metastatic regions of dissected lymph nodes. , 2012, , .		5
59	Liver Stiffness: A Significant Relationship with the Waveform Pattern in the Hepatic Vein. Ultrasound in Medicine and Biology, 2015, 41, 1801-1807.	1.5	5
60	Development of a viscoelastic phantom for ultrasound and MR elastography satisfying the QIBA acoustic specifications. , 2020, , .		5
61	Characterization of blood mimicking fluid with ultrafast ultrasonic and optical image velocimeters. Japanese Journal of Applied Physics, 2022, 61, SG1067.	1.5	5
62	Shear wave speed measurement bias in a viscoelastic phantom across six ultrasound elastography systems: a comparative study with transient elastography and magnetic resonance elastography. Journal of Medical Ultrasonics (2001), 2022, 49, 143-152.	1.3	5
63	Application of Ultrasonic Microscopy to Evaluation of Electrically Ligated Vessel Tissue. Japanese Journal of Applied Physics, 2013, 52, 07HF20.	1.5	4
64	Non-Invasive Diagnosis of Portal Hypertensive Gastropathy: Quantitative Analysis of Microbubble-Induced Stomach WallÂEnhancement. Ultrasound in Medicine and Biology, 2016, 42, 1792-1799.	1.5	4
65	Quantifying scattering from dense media using two-dimensional impedance maps. Journal of the Acoustical Society of America, 2020, 148, 1681-1691.	1.1	4
66	Backscatter properties of two-layer phantoms using a high-frequency ultrasound annular array. Japanese Journal of Applied Physics, 2022, 61, SG1049.	1.5	4
67	Three-dimensional quantitative high-frequency characterization of freshly-excised human lymph nodes. , 2011, , .		3
68	Evaluation of fibrotic probability image by multi-Rayleigh model for ultrasound image of liver using automatic region of interest selection. , 2015, , .		3
69	Free fatty acid-based low-impedance liver image: a characteristic appearance in nonalcoholic steatohepatitis (NASH). European Radiology Experimental, 2020, 4, 3.	3.4	3
70	In Vivo Quantitative Ultrasound on Dermis and Hypodermis for Classifying Lymphedema Severity in Humans. Ultrasound in Medicine and Biology, 2022, 48, 646-662.	1.5	3
71	Evaluation of contrast enhancement ultrasound images of Sonazoid microbubbles in tissue-mimicking phantom obtained by optimal Golay pulse compression. Japanese Journal of Applied Physics, 2022, 61, SG1015.	1.5	3
72	Lymph Explorer: A new GUI using 3D high-frequency quantitative ultrasound methods to guide pathologists towards metastatic regions in human lymph nodes. , 2012, , .		2

Тадазні Үамадисні

#	Article	IF	CITATIONS
73	Three-dimensional quantitative ultrasound to guide pathologists towards metastatic foci in lymph nodes. , 2012, 2012, 1114-7.		2
74	3D ultrasound assisted laparoscopic liver surgery by visualization of blood vessels. , 2013, , .		2
75	Analysis of mechanical and biological effects of ultrasonically activated devices. Acoustical Science and Technology, 2015, 36, 182-185.	0.5	2
76	Effects of Signal Saturation on QUS Parameter Estimates Based on High-Frequency-Ultrasound Signals Acquired From Isolated Cancerous Lymph Nodes. IEEE Transactions on Ultrasonics, Ferroelectrics, and Frequency Control, 2017, 64, 1501-1513.	3.0	2
77	Development of a poly (vinyl alcohol) hydrogel phantom to allow physical measurement in ultrasonographic conditions: A model for scatter. , 2017, , .		2
78	Size-dependent translational velocity of phospholipid-coated bubbles driven by acoustic radiation force. Japanese Journal of Applied Physics, 2022, 61, SG1018.	1.5	2
79	Quantification of the scatterer distributions for liver fibrosis using modified Q-Q probability plot. , 2014, , .		1
80	Comparison of modeling accuracy of amplitude distribution models for ultrasonic tissue characterization of liver fibrosis. , 2016, , .		1
81	Compensating effect of minor portal hypertension on the muscle mass loss-related poor prognosis in cirrhosis. International Journal of Medical Sciences, 2017, 14, 804-810.	2.5	1
82	Quantitative Evaluation Method for Liver Fibrosis in Clinical Ultrasound B-Mode Image Based on Optimized Multi-Rayleigh Model. , 2018, , .		1
83	Image feature conversion of pathological image for registration with ultrasonic image. , 2018, , .		1
84	A method of visualizing the three-dimensional fiber tissue structure in diffuse liver diseases. Choonpa Igaku, 2009, 36, 59-61.	0.0	1
85	Multi-scale speed of sound analysis by comparing of histological image and ultrasonic microscopic images at multiple frequencies. , 2019, , .		1
86	Quantitative Estimation of Diffused Liver Diseases Using Ultrasound Echo Signal. Key Engineering Materials, 2004, 270-273, 2085-2092.	0.4	0
87	Speckle removal from heterogeneous-tissue signals using independent component analysis. , 2009, , .		Ο
88	Multi modality fusion imaging technique for laparoscopic surgery guiding. , 2011, , .		0
89	Comparison of acoustic properties in various rat organs using high frequency ultrasound. , 2014, , .		Ο
90	Notice of Removal: Effect of multi-reflection on analysis of acoustic impedance of cultured cells. , 2017, , .		0

Тадазні Үамадисні

#	Article	IF	CITATIONS
91	Structure factor model-based approach for analyzing two-dimensional impedance map and studying scattering from polydisperse dense media. , 2017, , .		0
92	Structure factor model-based approach for analyzing two-dimensional impedance map and studying scattering from polydisperse dense media. , 2017, , .		0
93	Destruction of giant cluster-like vesicles assisted by contrast agent under 2.8-MHz ultrasound irradiation. , 2017, , .		0
94	Verification of Error Factors and Accuracy Improvement in Speed of Sound Analysis at Ultra-High Frequency. , 2018, , .		0
95	The Speed of Sound Analysis from Micro to Macro Size by Wide Area Ultrasound Microscopic Measurement. , 2018, , .		0
96	Visualization of a simulated lymph channel using contrast enhanced active Doppler ultrasonography method. , 2019, , .		0
97	Analysis of fluctuation for pixel-pair distance in co-occurrence matrix applied to ultrasonic images for diagnosis of liver fibrosis. Choonpa Igaku, 2021, 48, 3-15.	0.0	0
98	Verification of Ultrasonic Image Fusion Technique for Laparoscopic Surgery. Japanese Journal of Applied Physics, 2012, 51, 07GF04.	1.5	0
99	2A07 The ultrasonic comprehensive diagnosis/treatment assistive technology of alimentary. The Proceedings of the Bioengineering Conference Annual Meeting of BED/JSME, 2013, 2013.25, 245-246.	0.0	0
100	2B31 Laparoscopic ultrasound and endoscopic image overlay system using probe angle detection. The Proceedings of the Bioengineering Conference Annual Meeting of BED/JSME, 2014, 2014.26, 313-314.	0.0	0
101	2B45 Analysis for acoustic characteristics of rat organs using bio-acoustic microscopy. The Proceedings of the Bioengineering Conference Annual Meeting of BED/JSME, 2014, 2014.26, 333-334.	0.0	0
102	2B44 Tissue Characterization using High-frequency Ultrasound Scanner. The Proceedings of the Bioengineering Conference Annual Meeting of BED/JSME, 2014, 2014.26, 331-332.	0.0	0
103	Local Changes in 90Sr Deposition in the Soil as Observed in Hokkaido Island, Japan. Journal of Radiation Research, 1961, 2, 20-24.	1.6	0